Spiking Neuron Models of the Medial and Lateral Superior Olive for Sound Localisation

Julie A. Wall, Liam J. McDaid, Liam P. Maguire and Thomas M. McGinnity

Abstract—**Sound localisation is defined as the ability to identify the position of a sound source. The brain employs two cues to achieve this functionality for the horizontal plane, interaural time difference (ITD) by means of neurons in the medial superior olive (MSO) and interaural intensity difference (IID) by neurons of the lateral superior olive (LSO), both located in the superior olivary complex of the auditory pathway. This paper presents spiking neuron architectures of the MSO and LSO. An implementation of the Jeffress model using spiking neurons is presented as a representation of the MSO, while a spiking neuron architecture showing how neurons of the medial nucleus of the trapezoid body interact with LSO neurons to determine the azimuthal angle is discussed. Experimental results to support this work are presented.**

I. INTRODUCTION

OF all the organs in the body, there are very few that can compare to the ear with regards to the degree of functionality it contains within such a small and compressed space. Sound localisation is one function that the ears perform, defined as determining where a sound signal is generated in relation to the position of the human head. It is a very powerful aspect of mammalian perception, allowing an awareness of the environment and permitting mammals to locate prey, potential mates and to determine from where a predator is advancing [1].

Mammalian sound localisation is determined with a combination of ITD for low frequency sound-signals (less than 1.5 KHz in humans) and IID for high frequencies. ITD can be defined as the very small difference in arrival times between a sound-signal reaching each individual ear [2]. From this difference, the brain can calculate the angle of the sound source in relation to the head [3], [4]. ITD is very sensitive and can differentiate between angles of only 1-2° [2]. It is calculated in the MSO, the largest of the nuclei in the superior olivary complex (SOC); the human MSO contains between 10,000-11,000 cells [5], [6]. The pathways the sound signals take from each ear begin at the cochlea; exiting the cochlea they are encoded as spike trains and travel up the auditory nerve to the spherical bushy cells of the anteroventral cochlear nucleus (AVCN) which phase-lock the sound signal they are transmitting and finally enter

The authors are with the Intelligent Systems Research Centre (ISRC), School of Computing and Intelligent Systems, Faculty of Computing and Engineering, Magee Campus, University of Ulster, Northland Road, Derry, Northern Ireland, BT48 7JL, UK. (phone: +44 (0)28 71375166; email: wall-j@ulster.ac.uk).

the MSO as an excitatory innervation, see Fig. 1. MSO cell types are primarily excited - excited (EE), i.e. they receive excitatory innervation from both ears, and their main functionality is to work as coincidence detectors to identify the ITD and thus the sound source angle [7]. The MSO combines the sound from the two ears; the ipsilateral inputs come directly while the contralateral inputs pass through a graded series of delays. For a sound source at a particular angle to the listener, only one delay will allow the ipsilateral and contralateral inputs to arrive coincidentally at the neuron or group of neurons, thus causing the neuron to fire. MSO neurons are organised spatially as a place map of location, i.e. a group of neurons are allocated for each particular angle on the horizontal plane [3], [8], [9].
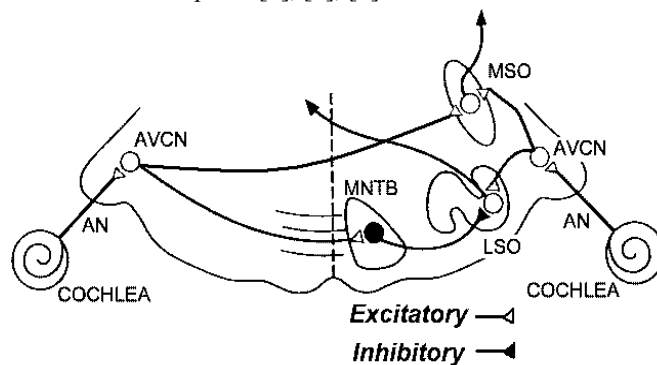

Fig. 1. ITD and IID pathway of the biological auditory system [10]

IID can be defined as the difference in sound pressure levels (SPL) of the sound signal between each ear [10] and is computed in the LSO of the SOC (Fig. 1). The LSO is significantly smaller than the MSO with only about 2,500-4,000 cells in the human LSO [6]. It appears as a folded sheet of excited-inhibited (EI) neurons; excited by innervation from spherical bushy cells of the ipsilateral AVCN but inhibited by innervation from the medial nucleus of the trapezoid body (MNTB) which receives input from globular bushy cells of the AVCN [8]. For high frequency sound waves that have a similar or smaller wavelength than the diameter of the head, a shadowing effect will occur on the sound wave that approaches the ear furthest from the sound, see Fig. 2. This shadowing of the sound wave gives a difference of intensity between the two sound signals for each ear and the resulting encoded signals will also differ. The excitatory stimulus from one ear passes through the cochlea to the AVCN and up the auditory pathway, now in the encoded form of spike trains, to the LSO. The excitatory

stimulus from the other ear again travels through the cochlea to the AVCN but enters the MNTB. The MNTB is the smallest nucleus of the SOC and takes excitatory input from the contralateral AVCN globular bushy cells which phase-lock the sound signal. Acting as a simple relay it passes the signal through an inhibitory synapse on the LSO converting it to an inhibitory stimulus [11]. Here, the post-synaptic potential (PSP) of the stimulus from one ear is subtracted from the PSP from the other ear, giving a neural significance corresponding to the IID [10].

Sound localisation processing is achieved in real time as the brain utilizes parallel processing using many neurons to simultaneously transmit the information up through the auditory pathway; the number of neurons varies from six to forty for each one-third-octave frequency band [13].
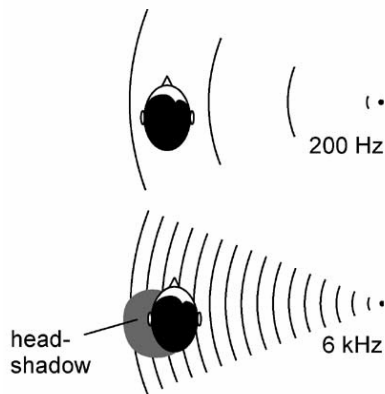
Fig. 2. Low and high frequency sound signals showing head shadow effect [12]

In this paper spiking neurons are configured to model the primary function of the MSO and LSO. The paper presents an implementation of the Jeffress model [14] using spiking neurons where it is shown that after a period of training, the activity of the output neurons can be associated with an azimuth angle: the training algorithm uses the conventional STDP rule. The LSO is modelled using a spiking LSO neuron to compute the difference in the frequency of spike trains from each cochlea to reflect the IID.

Section II provides a review of the related research conducted in the field. Section III outlines the MSO and LSO architectures with supporting experimental results while section IV concludes the paper.

II. LITERATURE REVIEW

Research relevant to this work ranges over fifty years and the topics of research also differ rather significantly. In 1948, Jeffress created the first computational model (Fig. 3) to show how ITD works in mammals to determine the angle of origin of a sound signal [3], [14]. His model involved time or phase locked inputs; a set of delay lines to vary the axonal path lengths arriving at the neuron and an array of coincidence detector neurons which only fire when presented with simultaneous inputs from both ears [1], [3], [4], [5].

Coincident inputs only occur when the ITD is exactly compensated for by the delay lines. The fundamental importance of Jeffress' model, and why it is has become the prevailing model of binaural sound localisation, is its ability to depict auditory space with a neural representation in the form of a topological map, even though Jeffress himself acknowledged the simplicity of his model [1].
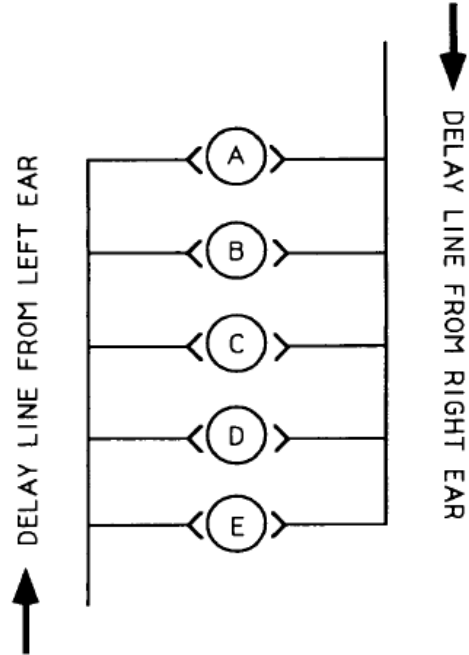

Fig. 3. The Jeffress (1948) computational model [14]

Schauer et al. [15] have based their work extensively on the Jeffress sound localisation model. Their initial research involved a biologically inspired model of binaural sound localisation again by means of ITD; using a spike response model for implementation in analog VLSI. Slight modifications to the Jeffress model were made including a digital delay line with AND gates. Data recorded in an open environment was used in offline testing and results showed that the model was proficient at localising single sound sources for sixty-five azimuthal angles. Schauer and Gross [16] extended this work to discriminate between sound sources of different orientations. However, this was achieved in a biologically implausible way. The authors simply specified one microphone for the front and another for the back. Differences in the sound colour of the binaural signals, calculated using a short-term Fast Fourier Transform (FFT), determined from which direction the sound approached. Again positive results were achieved during testing in open environments, including a lecture hall and a shopping centre. Similar to Schauer, Shi and Horiuchi [9] focused on one part of the superior olivary complex to develop a model of sound localisation. They created a CMOS VLSI circuit to imitate the functionality of ILD in the bat LSO. Their hardware system included a spike generator which provided input to the LSO spike response model and a post-processor to extract azimuth information from the outputs of the LSO

model. Experimental results after chip testing showed that their system effectively captured IID computation in the bat LSO.

Other researchers have also included models of both the MSO and LSO in their work. Kuroyanagi and Iwata [17] developed a neural network for localising sound which involved both an MSO and LSO model. Their model consisted of a cochlear filter and hair cell models which processed the inputs, an auditory nerve model for converting the inputs to pulse trains and a pulse neuron model implementation of both the MSO and LSO. Based on input data of white noise with Gaussian distributed amplitudes they were able to determine the ITD and IID values. Similarly, Willert et al. [12] proposed a biologically inspired sound localisation system to provide an approximation of the angle of a sound source. Binaural cues produced by a cochlear model are used as inputs to the system which independently measured IIDs and ITDs. Based on these measurements, a probabilistic evaluation determined the position of the sound source. Although their model included some features of the biological equivalent such as the tonotopic mapping of ITDs and IIDs, they did not employ spiking neurons and instead used correlation and probabilistic-based methods. However, their results based on human speech signals showed a very high accuracy of up to 98.9%.

The development of a bio-inspired technique that can detect the location of sound is an active area of research. Many researchers have based their work on Jeffress' computational model of sound localisation. However, limited progress has been made regarding the development of a modified Jeffress architecture based on spiking neurons and in addition, more work is needed to develop a biologically plausible architecture for the LSO. This paper addresses these issues by implementing a Jeffress based model for the MSO using spiking neurons and with considerable background research on the biology of the auditory system, it also develops a model for the LSO. The remainder of this paper discusses the proposed MSO and LSO architectures.

III. Sound Localisation

A. MSO Architecture

The MSO architecture presented here represents an extension of earlier work [18] whereby a spiking neural network (SNN) implementation of Jeffress' architecture is extended to thirty-seven angles (every 5°) on the horizontal azimuthal plane. The architecture (Fig. 4) consists of thirty-seven processing neurons implemented using the leaky integrate and fire (LIF) model which replicate the coincident-detection neurons of the MSO [19]. The inputs $t1$ and $t2$ (chosen arbitrarily) correspond to the length of time taken for the sound to reach both cochleas, and these inputs are passed to the processing neurons via the cochlear nodes. The synapse on each pathway encompasses a multiple delay structure similar to the graded series of delays found in the
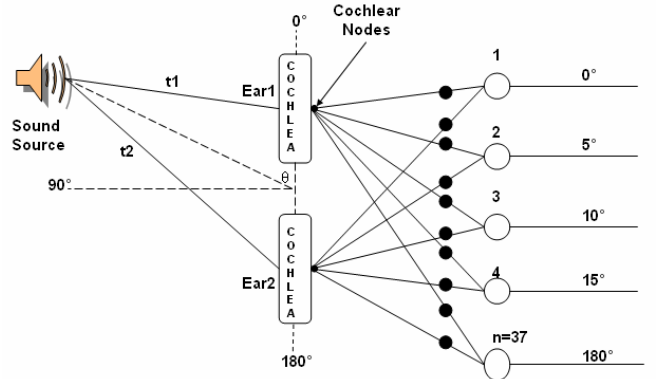
biological MSO, see Fig. 5.

Fig. 4. Spiking neural network architecture of the MSO model. LIF parameters are: voltage threshold Vth = 6 V, refractory period tref = 2 ms, voltage reset Vreset = 0 V,. Synapses: initial membrane voltage Vinit = 0 V; time constant τ = 4.5 ms.

Fig. 5 shows how delay lines are used in this model, where t_{pre} is the presynaptic spike time; d_m are the axonal delays; w_m are the weights; and t_{post} is the postsynaptic spike time [20]. The output spike from neuron A is passed to m (=37) interneuron connecting pathways, each with their own weight w_m.
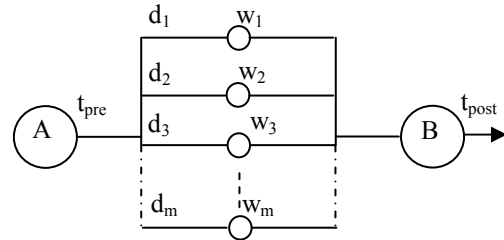

Fig. 5. Pre and post synaptic neurons with interconnecting delay lines [20]

Spike timing dependent plasticity (STDP) was used for training the Jeffress network by selecting the optimal delay line to facilitate coincidence. STDP occurs naturally in neurons and is a form of synaptic plasticity, i.e. the capacity for the synapse connecting two neurons to change strength [21]. It is a form of Hebbian learning which strengthens the weights of the synapses that are activated before the post synaptic spike and weakens those synaptic weights that are activated after the post synaptic spike [22], [23]. The weight updates are potentiated according to:

$$\delta w_i = A_1 e^{\frac{-\delta t_i}{\tau_1}} \qquad (1)$$

and depressed according to:

$$\delta w_i = -A_2 e^{\frac{\delta t_i}{\tau_2}} \qquad (2)$$

where δw_i is the weight change, A_1 is the maximum value of the weight potentiation, A_2 is the maximum value of weight depression, δt_i is the difference between the input and output

spike times, and τ_1 and τ_2 reflect the width of the window for long term potentiation and depression respectfully.

For this work single spike encoding is used where the single sound source was assigned arbitrarily chosen values of *t1* and *t2* to represent the signal delay at each ear, as a function of angle (see Fig. 4). Each output neuron was trained to recognise different delay values (*t1,t2)* representing different angles in the azimuthal plane. Each 5° angle was assigned unique delay values and consequently there were 37 training sets. Table 1 shows a sample of these with arbitrarily chosen output firing times: parameters for training the first five output neurons with their associated angles where *tOut* is the desired post synaptic spike time.

TABLE I
TRAINING PARAMETERS

θ	t1	t2	tOut
0°	1	37	38
5°	2	36	39
10°	3	35	40
15°	4	34	41
20°	5	33	42

Supervised training is used in this work where each delay set is passed to the network and the weight values for each neuron are calculated, using equations (1) and (2). For the delay lines which caused coincidence at the neuron, STDP increased their weights according to the learning rule in (1) and the weights of the other delay lines are decreased according to (2): parameters for the learning rule in (1) and (2) are: $A_1 = A_2 = 0.5$ and $\tau_1 = \tau_2 = 4.5$ ms. The neurons corresponding to each of the thirty-seven angles were passed inputs *t1* and *t2*, and after training the classifying neuron for each angle will only fire when presented with their unique inputs. After a period of training (40 epochs) the ITD encoded in *t1*/*t2* is compensated for through selection of the appropriate delay lines using STDP and the pre-selected output neurons fires. Other inputs will also have reached the neuron but due to the training procedure their combined post-synaptic potentials (PSP) will not be sufficient to cause coincidence at the neuron, and therefore it remains silent.

The graph in Fig. 6 shows the weight distribution on the vertical axis of the post trained SNN where each window 1 to 5 represents the first five classifying neurons and their associated weights: the horizontal axis is the spatial distribution of synapses across the network. The dotted line at a weight value of 0.5 represents the pre-trained weight distribution. It is important to note the bimodal weight distribution which is characteristic of the STDP process. Potentiated weights at approximately 2.5 are associated with pathways that have been selected by the STDP training rule because their delays cause coincidence at the appropriate classifying neuron.

The test data consisted of both the training data and randomly selected values for *t1* and *t2*. In all cases, the Jeffress model presented here was able to make an accurate classification on all the input data, i.e. each neuron classified to their own respective outputs with 100% accuracy. To increase the architecture to classify down to 1-2° would merely involve increasing the number of neurons in the output layer. Performance does not break down at the 5° threshold as there is no fundamental limit on angle; only the size of the network will be affected as in this architecture the number of processing neurons is directly dependent on the resolution of the localisation angle. Finally, this research used synthetic arbitrarily chosen training and testing data and further work will verify our Jeffress network using a more realistic data set [24], [25].
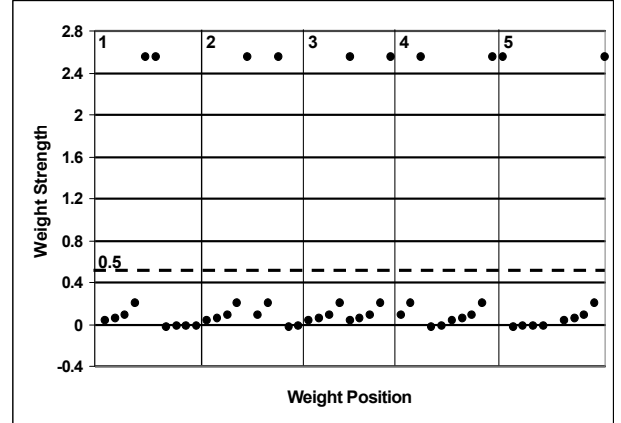

Fig. 6. Bimodal distribution of weights after training for the first five classifying neurons

B. LSO Architecture

Consider the proposed LSO architecture in Fig. 7 stimulated by a single sound source *S* at an angle *θ*. The sound reaches the cochlea of the ipsilateral ear1 with a Sound Pressure Level (SPL) of *E1* and the contralateral ear2 with an SPL of *E2*. The cochlea maps each SPL to a spike train at its output: *E1* maps to a spike train at the output *C1* and *E2* to *C2*. The output spike train at *C1* from the ipsilateral ear stimulates an LSO neuron, where the frequency sensitive receptive field associated with the interconnecting excitatory synapse will route the train to this neuron. The output spike train at *C2* from the contralateral ear stimulates each MNTB neuron; no frequency sensitive receptive fields are placed on the interconnecting excitatory synapses. Each MNTB neuron then stimulates an inhibitory synapse of all LSO neurons in the network. Note that each LSO neuron is responsive to the different sound intensities associated with the source S: finite intensity ranges are captured in the frequency bands which are determined by the frequency sensitive receptive field from the ipsilateral ear. The difference in the frequencies at outputs C1 and C2 within each band is used to determine θ. The LSO neurons in layer two compute the differential in frequency of the combined inputs from the ipsilateral and contralateral ears. To calculate the differential the excitatory PSP and inhibitory PSP are summed; essentially the inhibitory PSP generates the neural equivalent of subtraction. The resultant

PSP generated from this summation is the input to the LSO neuron causing it to fire. In this network each of the output frequencies from LSO neurons are allocated a different angle on the horizontal plane. Therefore, the outputs from the LSO neurons are routed by receptive fields, allowing only a pre-defined frequency to arrive at each output neuron. Similar to the MSO model, whichever output neuron fires for each frequency band will determine the angle of location of the sound source.
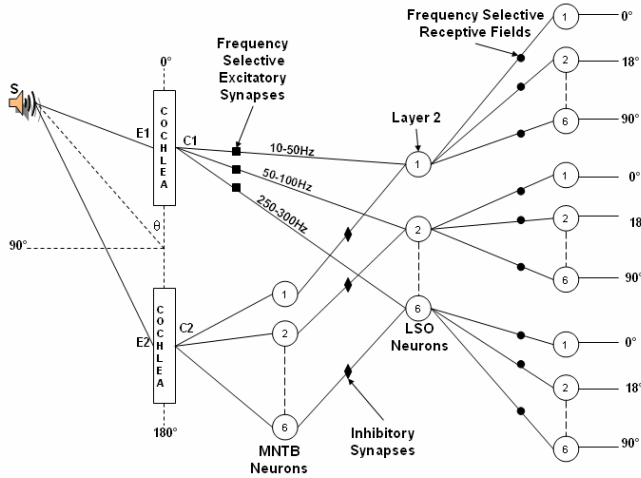

Fig. 7. Proposed LSO architecture consisting of a three-layered spiking neural network

The remainder of the paper considers how a spiking neuron model for the LSO implemented with the LIF neuron model can relate the frequency at its output f_o to the differential of the input spike train frequencies f_1 and f_2 (Fig 8).
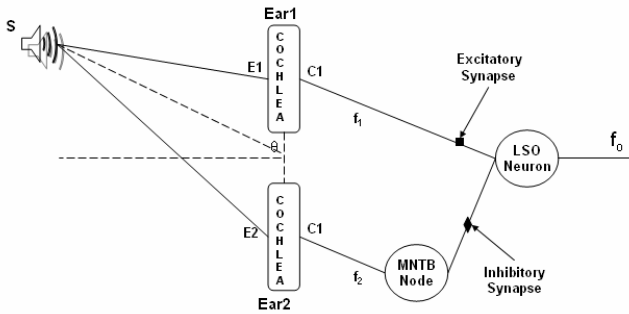

Fig. 8. LSO neuron model to compute the differential of the inputs from the excitatory and inhibitory synapses. LIF parameters are: voltage threshold Vth = 2.5 V, refractory period tref = 1 ms, voltage reset Vreset = 0 V. Synapses: initial membrane voltage Vinit = 0 V, time constant τ = 37 ms.

The parameters for both the neuron and synapse were chosen by fine-tuning the neuron model to achieve appropriate frequency ranges at the output f_0. Recall that the frequency of each spike train at C1 and C2 reflects the SPL at each ear of a single frequency sound signal at different angles in the horizontal plane: in our experiments f_1 was fixed and f_2 was varied. f_1 is passed directly to the excitatory synapse of the LSO neuron while f_2 passes through the MNTB node to an inhibitory synapse associated with the LSO neuron. The associated inhibitory response is therefore

subtracted from the excitatory PSP producing a stimulus for the LSO neuron that reflects the frequency difference.

Therefore, the LSO neuron generates an output frequency f_o which is a measure of the difference between the two input frequencies, f_1 and f_2. f_o is a key component in the way the LSO determines the azimuthal angle of the sound signal as the range of output frequencies can be mapped to the range of angles on the horizontal azimuthal plane [26]. When the LSO neuron produces no output, i.e. $f_o = 0$, it can be concluded that the sound signal is at 90°; the sound reaches both ears at the same time so both f_1 and f_2 have the same encoded frequency and the IID is 0. As the IID increases, f_o will also increase as the angle of the sound source tends towards 0°. Fig. 9 shows Matlab plots illustrating how different combinations of spike train frequencies at C1 and C2 cause different output frequencies, f_o, at the LSO neuron. The excitatory frequency of 100Hz and the two inhibitory frequencies of 80Hz and 90Hz were chosen arbitrarily for the purpose of demonstrating the system. The output frequencies were determined by counting the number of spikes in the spike train for stimulus duration of 1s.
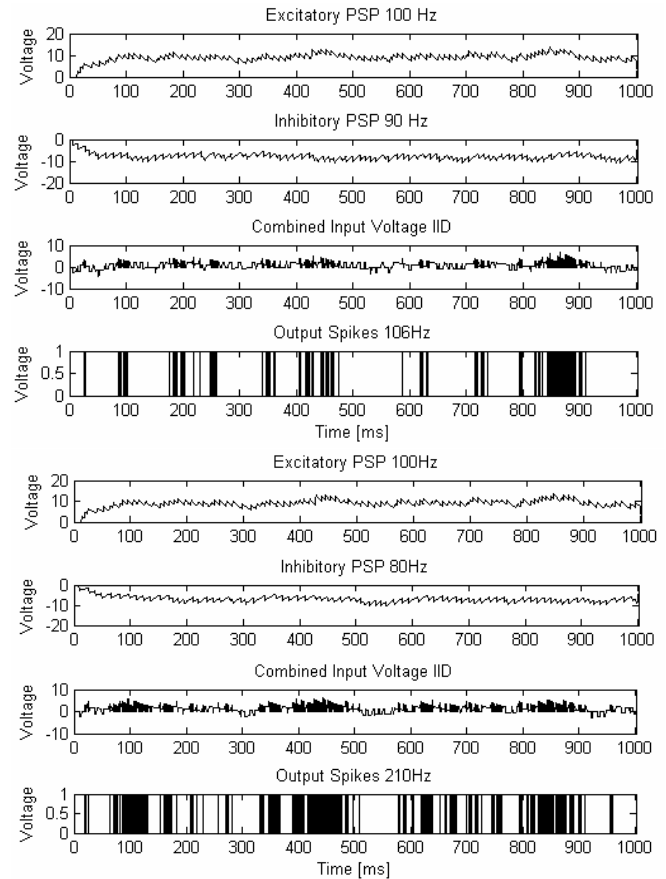

Fig. 9. Matlab plot of LSO model with an inhibitory and excitatory input frequency, their combined PSP and the resulting output frequency

The LSO model was tested with ten sets of input frequencies. Each test set had reflected a different IID in the frequency of the spike trains. Frequency f_1 was fixed at 100Hz while f_2 was varied over a range 10Hz – 100Hz: the

authors are aware that high frequencies are more typically associated with the LSO; however for the initial experiments on the one neuron LSO model, low frequencies reduced the complexity of the inputs. Additionally, when scaling up to the proposed LSO network architecture, input frequencies will be in the range of 600 – 30,000 Hz. With $f_1=f_2$, the LSO neuron produced no output spikes. As the inhibitory frequency was reduced for each subsequent test set, the output frequency increased, as expected. Fig. 10 shows the relationship between the LSO neuron output frequency f_o and the differential of its inputs f_1 and f_2. It can be seen that as the differential of the input frequencies changes the firing rate of the LSO neuron also changes. It should be pointed out that the LSO neuron model presented here had fixed weight values as no training took place. Training was not necessary for this initial neuron model as this work was carried out for the purpose of demonstrating the combination of an inhibitory and excitatory PSP and how their differential when inputted to a neuron produces a significant output frequency that can be used for sound localisation. However, the relationship between f_o and the differential between the input spike trains, f_1 and f_2, could be altered by selectively adjusting the weight values for both the inhibitory and excitatory synapses. This could then be used to map f_o to azimuthal angles for the purpose of sound localisation. Moreover, the relationship between the SPL at each ear and the encoded spike train frequencies at $C1$ and $C2$ will need to be determined in order to relate the output frequency of the LSO neuron to an accurate angle of location for the sound source.
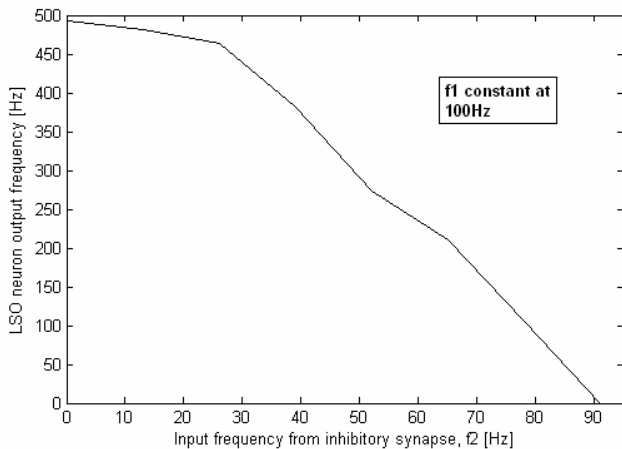

Fig. 10. Mapping of LSO output frequency to the differential of the input frequencies f_1 and f_2.

IV. DISCUSSION

The proposed Jeffress-based model consists of thirty-seven processing neurons implemented using the LIF neuron model which replicate the coincident-detection neurons of the MSO. The synapse on each pathway to the processing neurons encompasses a multiple delay structure similar to the graded series of delays found in the biological MSO. STDP was used for training the network by selecting the optimal

delay line to facilitate coincidence. The topology of the architecture allocates a processing neuron for each range of localised angles, i.e. to localise to a 1° accuracy would involve having 181 (0° - 180°) processing neurons in the network. Currently the network localises to 5° accuracy with 37 processing neurons in the output layer. To boost the accuracy of the network would involve increasing the complexity; however this complexity can be seen in the biological MSO which consists of about 10,000 neurons.

The second model outlines how LIF neurons can be employed to emulate the functionality of the LSO, i.e. how the frequency of the output can be related to the IID (differential of the inhibitory and excitatory input spike train frequencies). This is a key component in the way the LSO determines the azimuthal angle of the sound signal as the range of output frequencies can be mapped to the range of angles on the horizontal azimuthal plane. A three-layered spiking neural network is proposed for the architecture of the LSO whereby each LSO computes over a band of frequencies selected. Results show that the output firing frequency is related to differential in the input spike trains.

The main inadequacy of the MSO model is the single spike encoding of inputs. When more realistic data becomes available, it will have to be encoded as single spikes to ensure that comparisons can be made to the results outlined in this paper. As the inputs to the LSO model are encoded as spike trains and a binaural sound localization model would entail a combination of both MSO and LSO models; it would be beneficial for both to employ similar input encoding.

The limitation of the current LSO one neuron model is its implementation based on arbitrarily chosen input data. Also, presently the output frequencies of the LSO model cannot be mapped to an accurate angle of location, as the relationship between the SPL at each ear and the encoded spiked train frequencies were not known at the time of implementation. However, these restrictions in the model will be overcome by the proposed LSO network model which will be implemented based on more realistic data [24], [25].

V. CONCLUSION

This paper proposes simple models for the sound localisation process of the brain. Both areas of the auditory pathway, the MSO and LSO, which provide this functionality were implemented using spiking neurons based on the LIF neuron model. The MSO model involved an implementation of the Jeffress model using spiking neurons and successfully localised to every 5° on the horizontal azimuthal plane; while the LSO model employed a spiking neuron that could relate the frequency differential of its input frequencies to an output frequency. Future work will include implementing the proposed LSO architecture by extending the current neuron model. This will then be combined with the MSO model to provide a biologically inspired spiking neural network of binaural sound localisation based on the functionality of the superior olivary complex of the brain. Once this has been achieved, the model can be expanded upon to localise both more complex and multiple sound sources.

REFERENCES

[1] D. McAlpine and B. Grothe, "Sound Localization and Delay Lines – Do Mammals Fit the Model?", *Trends in Neurosciences*, vol.26, no. 7, pp.347 – 350, 2003.

[2] M. S. Lewicki, (2006) Sound Localization I. Available: http://www.cs.cmu.edu/~lewicki/cpsa/sound-localization1.pdf.

[3] B. Grothe, "New Roles for Synaptic Inhibition in Sound Localization", *Nature Reviews Neuroscience*, vol. 4, no. 7, pp 540 – 550, 2003.

[4] C. E. Carr, "Delay Line Models of Sound Localization in the Barn Owl", *American Zoologist*, vol. 33, no. 1, pp 79 – 85, 1993.

[5] M. Alexander, (2000) Sound Localization of Humans. Available: http://psy.ucsd.edu/~dmacleod/159/presentations05/MichaelSound%2 0Localization%20of%20Humans.ppt.

[6] J. K. Moore, "Organization of the Human Superior Olivary Complex", *Microscopy Research and Technique*, vol. 51, no. 4, pp 403 – 412, 2000.

[7] B. Delgutte and A. Oxenham, (2005) Hearing and the Auditory System: Overview. Available: http://ocw.mit.edu/OcwWeb/Health-Sciences-and-Technology/HST-725Spring2004/LectureNotes/index.htm.

[8] (2002), Auditory II: Central Mechanisms. Available: http://www.uphs.upenn.edu/audres/id110cen.htm.

[9] R. S. Shi and T. K. Horiuchi, "A VLSI Model of the Bat Lateral Superior Olive for Azimuthal Echolocation", in *Proc. of the International Symposium on Circuits and Systems*, vol. 4, pp 900 – 903, 2004.

[10] D. J. Tollin, "The Lateral Superior Olive: A Functional Role in Sound Source Localization", *The Neuroscientist*, vol. 9, no. 2, pp 127 – 143, 2003.

[11] B. Grothe and T. J. Park, "Structure and Function of the Bat Superior Olivary Complex", *Microscopy Research and Techniques*, vol. 51, no. 4, pp 382 – 402, 2000.

[12] V. Willert, J. Eggert, J. Adamy, R. Stahl and E. Körner, "A Probabilistic Model for Binaural Sound Localization", in *Proc. of IEEE Transactions on Systems, Man and Cybernetics – Part B*, vol. 36, no. 5, pp 982 – 994, 2006.

[13] W. M. Hartmann, (1999) "How We Localize Sound", *Physics Today on the We*b. Available: http://www.aip.org/pt/nov99/locsound.html.

[14] L. A. Jeffress, "A Place Theory of Sound Localization", *Journal of Comparative Physiology and Psychology*, vol. 41, no. 35 – 39, 1948.

[15] C. Schauer, T. Zahn, P. Paschke and H. M. Gross, "Binaural Sound Localization in an Artificial Neural Network", in *Proc. of the IEEE International Conference on Acoustics, Speech and Signal Processing (ICASSP)*, vol. 2, pp 865 – 868, 2000.

[16] C. Schauer and H. M. Gross, "Model and Application of a Binaural 360° Sound Localization System", in *Proc. of the International Joint Conference on Neural Networks*, vol. 2, pp 1132 – 1137, 2001.

[17] S. Kuroyanagi and A. Iwata, "Perception of Sound Direction by Auditory Neural Network Model using Pulse Transmission – Extraction of Inter-aural Time and Level Difference", in *Proc. of the International. Joint Conference on Neural Networks*, vol. 1, pp 77 – 80, 1993.

[18] J. Wall, L. J. McDaid, L. P. Maguire and T. M. McGinnity, "A Spiking Neural Network Implemenation of Sound Localization", in *Proc. of the Irish Signals and Systems Conference (ISSC)*, pp 19 – 23, 2007.

[19] B. Ibarz, H. Cao and M. A. F. Sanjuan, "Map-Based Neuron Networks", *Cooperative Behaviour in Neural Systems: Ninth Granada Lectures*, vol. 887, pp 69 – 76, 2007.

[20] T. J. Strain, L. J. McDaid, L. P. Maguire and T. M. McGinnity, "A Novel Mixed Supervised-Unsupervised Training Approach for a Spiking Neural Network Classifier", in *Proc. of the IEEE SMC UK-RI Chapter Conference on Intelligent Cybernetic Systems*, pp. 202 – 206, 2004.

[21] S. M. Martin, P. D. Grimwood and G. M. Morris, "Synaptic Plasticity and Memory: An Evaluation of the Hypothesis", *Annual Review of Neuroscience*, vol. 23, pp 649 – 671, 2000.

[22] R. J. Vogelstein, F. Tenore, R. Philipp, M. S. Adlerstein, D. H. Goldberg and G. Cauwenberghs, "Spike Timing-Dependent Plasticity in the Address Domain", in *Advances in Neural Information Processing Systems 15*, 2003.

[23] E. M. Izhikevich and N. S. Desai, "Relating STDP to BCM", *Neural Computation*, vol. 15, pp 1511 – 1523, 2003.

[24] D. J. Tollin, "The development of the acoustical cues to sound location in cats", *Association for Research in Otolaryngology Abstract*, vol. 27, no. 161, 2004.

[25] D. J. Tollin, "Encoding of Interaural Level Differences for Sound Localization", in *The Senses: A Comprehensive Reference*, vol. 3, A. I. Basbaum, A. Kaneko, G. M. Shepherd, G. Westheimer, P. Dallos and D. Oertel, Ed. San Diego: Academic Press, 2008, p. 631-654.

[26] A. Solodovnikov and M. C. Reed, "Robustness of a Neural Network Model for Differencing", *Journal of Computational Neuroscience*, vol. 11, no. 2, pp 165 – 173, 2001.